Marshall University
Marshall Digital Scholar

Chemistry Faculty Research | Chemistry

2001

Halogen Oxidation Reactions of (C5Ph5)Cr(CO)3 and Lewis Base Addition To [(C5Ph5)Cr(μ-X)X]2: Electrochemical, Magnetic, and Raman Spectroscopic Characterization of [(C5Ph5)CrX2]2 and (C5Ph5)CrX2(THF) (X = Cl, Br, I). X-ray Crystal Structure of [(C5Ph5)Cr(μ-Cl)Cl]2

Marc A. Hutton
Marshall University

James C. Durham
Marshall University

Robert W. Grady
Marshall University

Brett E. Harris
Marshall University

Recommended Citation

Hutton, M. A.; Durham, J. C.; Grady, R. W.; Harris, B. E.; Jarrell, C. S.; Mooney, J. M.; Castellani, M. P.; Rheingold, A. L.; Kölle, U.; Korte, B. J.; Sommer, R. D.; Yee, G. T.; Boggess, J. M.; Czernuszewicz, R. S., Halogen Oxidation Reactions of (C5Ph5)Cr(CO)3 and Lewis Base Addition To [(C5Ph5)Cr(μ-X)X]2: Electrochemical, Magnetic, and Raman Spectroscopic Characterization of [(C5Ph5)CrX2]2 and (C5Ph5)CrX2(THF) (X = Cl, Br, I). X-ray Crystal Structure of [(C5Ph5)Cr(μ-Cl)Cl]2. Organometallics 2001, 20 (4), 734-740.

This Article is brought to you for free and open access by the Chemistry at Marshall Digital Scholar. It has been accepted for inclusion in Chemistry Faculty Research by an authorized administrator of Marshall Digital Scholar. For more information, please contact zhangj@marshall.edu, martj@marshall.edu.

Carter S. Jarrell
Marshall University

See next page for additional authors

Follow this and additional works at: http://mds.marshall.edu/chemistry_faculty

 Part of the Chemistry Commons

Authors
Marc A. Hutton, James C. Durham, Robert W. Grady, Brett E. Harris, Carter S. Jarrell, J. Matthew Mooney, Michael Castellani, Arnold L. Rheingold, Ulrich Kölle, Brenda J. Korte, Roger D. Sommer, Gordon T. Yee, J. Matthew Boggess, and Roman S. Czernuszewicz

This article is available at Marshall Digital Scholar: http://mds.marshall.edu/chemistry_faculty/21

Halogen Oxidation Reactions of $(C_5Ph_5)Cr(CO)_3$ and Lewis Base Addition To $[(C_5Ph_5)Cr(\mu\text{-}X)X]_2$: Electrochemical, Magnetic, and Raman Spectroscopic Characterization of $[(C_5Ph_5)CrX_2]_2$ and $(C_5Ph_5)CrX_2(THF)$ (X = Cl, Br, I). X-ray Crystal Structure of $[(C_5Ph_5)Cr(\mu\text{-}Cl)Cl]_2$

Marc A. Hutton, James C. Durham, Robert W. Grady, Brett E. Harris, Carter S. Jarrell, J. Matthew Mooney, Michael P. Castellani*

Department of Chemistry, Marshall University, Huntington, West Virginia 25755

Arnold L. Rheingold*

Department of Chemistry and Biochemistry, University of Delaware, Newark, Delaware, 19716

Ulrich Kölle*

Institute for Inorganic Chemistry, Technical University at Aachen, Prof.-Pirlet-Strasse 1, D-52074 Aachen, Germany

Brenda J. Korte, Roger D. Sommer, Gordon T. Yee*

Department of Chemistry and Biochemistry, University of Colorado, Boulder, Colorado, 80309

J. Matthew Boggess, Roman S. Czernuszewicz*

Department of Chemistry, University of Houston, Houston, Texas, 77204

Abstract

The 17-electron complex $(C_5Ph_5)Cr(CO)_3$ reacts with halogens ($C_6H_5I{\bullet}Cl_2$, Br_2, and I_2) in C_6H_6 to yield the dimeric oxidation products $[(C_5Ph_5)Cr(\mu\text{-}X)X]_2$ as thermally stable solids. Reactions with other chlorinating agents similarly yield $[(C_5Ph_5)CrCl_2]_2$. An X-ray crystal structure of $[(C_5Ph_5)Cr(\mu\text{-}Cl)Cl]_2$ was obtained. The magnetic properties of the Cl_2 bridged dimer have been determined and modeled using the usual isotropic hamiltonian $H = -2J\hat{S}_1 \bullet \hat{S}_2$ which yields J/k = –30 K. Low-temperature (77 K) Raman spectra of solid $[(C_5Ph_5)CrX_2]_2$ (X = Cl, I) allow assignments to be made for the metal-ring and metal halogen stretching modes in the low frequency region (< 600 cm^{-1}). Tetrahydrofuran (THF) cleaves these dimers to yield complexes of the form $(C_5Ph_5)CrX_2(THF)$.

Introduction

Over the past two decades, the study of paramagnetic organometallic complexes has greatly expanded.[1] These complexes are generally highly reactive and many have been postulated as reaction intermediates. In particular, the $(\eta^5\text{-}C_5R_5)Cr(CO)_3$ (R = H, Me, Ph) family of complexes recently has received much attention. The R = H and Me complexes both exist in equilibria between 17e monomers and 18e dimers in solution and as dimers in the solid state,[2] while for R = Ph the complex exists solely as a 17e monomer both in solution and the solid state.[3]

The isolation of $(C_5Ph_5)Cr(CO)_3$ allowed comparison of predicted and actual structural parameters, as well as a comparison of the physical properties of the three radical species $(C_5R_5)Cr(CO)_3$ (R = H, Me, Ph). In many ways the physical properties of these species are similar; however in some notable ways (e.g. reduction potentials) they differ significantly. A question that naturally follows such an examination is how the large size and electron-withdrawing capabilities of the pentaphenylcyclopentadienyl ligand affect the reactivity of complexes incorporating it.

Previous work has shown that reaction of the $[(C_5R_5)Cr(CO)_3]_2$ (R = H (Cp),[4] Me (Cp*)[5]) dimers with halogens yields complexes of the form $(C_5R_5)Cr(CO)_3X$ (X = Cl, Br, I). Likewise, Baird[5-8] and coworkers have shown that alkyl and allyl halides also produce $(C_5R_5)Cr(CO)_3X$ complexes. Herrmann and coworkers found that reacting excess chlorine or bromine with $[(C_5H_5)Cr(CO)_3]_2$ in acetonitrile yielded the complexes $CpCrX_2(CH_3CN)$ (X = Cl, Br).[9] Theopold and coworkers have prepared $[Cp^*Cr(\mu\text{-}X)X]_2$ by direct reaction of LiCp* with $CrCl_3\bullet 3THF$,[10] while several other methods have been reported by other groups.[11-15]

Interestingly, Fischer reports that allyl bromides convert $[CpCr(CO)_3]_2$ to $[CpCrBr_2]_2$ at elevated temperatures,[14] while Baird reports that alkyl and benzyl bromides react with $[CpCr(CO)_3]_2$ to yield $CpCr(CO)_3Br$ at or below ambient temperatures.[7] The two most reasonable pathways for $[CpCrX_2]_2$ formation are $CpCr(CO)_3X$ compounds decomposing or further reaction with RX. Although all known $(C_5R_5)Cr(CO)_3X$ complexes decompose slowly

both in solution and in the solid state, to our knowledge no determination of the decomposition products has been reported. Herein, we report the synthesis and characterization of $(C_5Ph_5)Cr(CO)_3X$ and $[(C_5Ph_5)Cr(\mu\text{-}X)X]_2$ (X = Cl, Br, I) compounds by a variety of pathways and show the halide bridged dimer results from the decomposition of the tricarbonyl halide in both solution and in the solid state.

Experimental Section

General Data. All reactions of air- and moisture-sensitive materials were performed under a nitrogen atmosphere employing standard Schlenk techniques unless otherwise stated. Solids were manipulated under argon in a Vacuum Atmospheres glovebox equipped with a HE-493 dri-train. Solvents (Fisher) were distilled from the appropriate drying agent under nitrogen: toluene, hexane (sodium/benzophenone), benzene, tetrahydrofuran (THF) (potassium/benzophenone), carbon tetrachloride, chloroform, and dichloromethane (CaH_2). $(C_5Ph_5)Cr(CO)_3 \bullet C_6H_6$[3] and $CrCl_3 \bullet 3THF$[16] were prepared according to literature procedures. NMR solvents were vacuum distilled from CaH_2 and placed under a nitrogen atmosphere. $C_6H_5I \bullet Cl_2$ was prepared following a literature procedure[17] and I_2 was sublimed prior to use. Br_2 (Fisher), $SOCl_2$ (Acros), PCl_3 (Mallinckrodt), and all other materials (Fisher) were used as received without further purification. Elemental analyses were performed by Mikroanalytisches Labor Pascher, Remagen, Germany.[18]

Electrochemistry. Cyclic voltammetry was performed with EG&G equipment (175 programmer and 173 potentiostat) as previously described[19] at a Pt electrode on 10^{-3} *M* substrate solutions in dichloromethane and THF using tetrabutylammonium hexafluorophosphate as the supporting electrolyte. Scan rates were generally 0.1 V s^{-1}. Data were stored on a Nicolet 3091 digital oscilloscope and transferred to a PC. Simulations were done with a Windows adaptation of the Gosser program.[20] The potential scale is vs. aqueous SCE, which is converted to the ferrocene scale by subtracting 0.40 V from the figures given.

Raman Spectroscopy. Raman spectra were obtained using a Coherent Innova 90–6 Ar^+ ion laser by collecting backscattered photons directly from the surface of a KCl–supported pellet held under vacuum in a liquid–N_2 dewar.[21] The radiation used was 514.5 nm. Laser power was varied from 150–400 mW. Under these conditions, no decomposition of the samples was observed. A Spex 1403 double monochromator equipped with a pair of 1800 grooves/mm holographic gratings and a Hamamatsu 928 photomultiplier detector was used to record the spectra under the control of a Spex DM3000 microcomputer system, as described in detail elsewhere.[22] Multiple scans (15–20) were averaged to improve signal to noise ratio. Each scan was obtained with 6–8 cm^{-1} slit widths at 1 cm^{-1}/s intervals. Manipulation of Raman data was performed using LabCalc software (Galactic Industries, Inc.).

Magnetic Susceptibility. Magnetization vs. temperature data were obtained on a Quantum Design MPMS 5T or 7T SQUID magnetometer in 1000 G applied field. Samples were loaded between two cotton plugs in gelatin capsules or in glass holders as previously described.[23] Diamagnetic corrections for the samples were calculated from Pascal's constants. The corrections for the holders were calculated from the measured average gram susceptibility of several nominally identical holders.

X-ray Structural Determination. Crystallographic data for $[(C_5Ph_5)Cr(\mu\text{-}Cl)Cl]_2 \bullet 2CH_2Cl_2$ are collected in Table 1. Dark green block crystals were photographically characterized and determined to belong to the triclinic crystal system. The centrosymmetric space group alternative was initially chosen by its frequency of occurrence and the distribution of *E* values; the choice was confirmed by subsequent refinement behavior. An empirical correction for absorption was applied to the data. The structure was solved by direct methods, completed from difference Fourier maps, and refined with anisotropic thermal parameters for all nonhydrogen atoms. Hydrogen atoms were placed in idealized positions, except for the disordered (two positions, 70/30 distribution) solvent molecule (CH_2Cl_2). All computations used SHELXTL (4.2) software (G. Sheldrick, Siemens XRD, Madison, WI).

$[(C_5Ph_5)Cr(\mu\text{-}Cl)Cl]_2$ (1). Method 1: $(C_5Ph_5)Cr(CO)_3$ (1.00 g, 1.72 mmol) was dissolved

in benzene (50 mL) and then transferred via cannula to a separate flask containing $C_6H_5I{\bullet}Cl_2$ (0.53 g, 2.02 mmol). The stirred solution immediately turned yellowish brown, then quickly to olive green with gas evolution. After stirring overnight, a green solid precipitated. The mixture was filtered via cannula and the solid dried *in vacuo* to yield 0.86 g (0.75 mmol, 88%) of **1** as an olive green powder. Crystals were grown by dissolving $(C_5Ph_5)CrCl_2(THF)$ (*vide infra*) in CH_2Cl_2 and layering with a 1:1 mixture of Me_3SiCl/hexane. mp: 335 °C (dec). Anal. Calcd for $C_{70}H_{50}Cl_4Cr_2$: C, 73.95; H, 4.43. Found: C, 73.55; H, 4.38.

Method 2: $Na[C_5Ph_5]$ (2.50 g, 5.34 mmol) and $CrCl_3{\bullet}3THF$ (2.00 g, 5.34 mmol) were combined in dry benzene (80 mL) to give a dark olive green colored solution. The mixture was refluxed overnight, cooled to room temperature, and filtered via cannula. The resulting solid was dried *in vacuo* to yield 2.13 g (1.87 mmol, 70%) of **1** as an olive green powder. The identity of the product in this reaction (and that in Method 3) was confirmed by comparison of its IR spectrum (KBr pellet) with that of a sample generated by Method 1.

Method 3: $(C_5Ph_5)Cr(CO)_3$ was dissolved in chloroform to give a blue solution. This reaction mixture was stirred overnight. Stirring was stopped and the suspended **1** was allowed to settle out.

$[(C_5Ph_5)Cr(\mu\text{-}Br)Br]_2$ (2): Bromine (0.082 mL, 3.18 mmol) was added to a stirred solution of $(C_5Ph_5)Cr(CO)_3$ (1.00 g, 1.72 mmol) in benzene (30 mL). The resulting reddish-brown solution changed to a dark olive green in *ca*. ten minutes. Stirring was stopped and a dark olive green solid precipitated. The mixture was filtered via cannula and the resulting solid was dried *in vacuo* to yield **2** (0.99 g, 87%) as an olive green powder. Visible (CH_2Cl_2) λ_{max} 410 (sh), 480 (sh), 655. mp: 330 – 333 °C (dec). Calcd for $C_{70}H_{50}Br_4Cr_2$: C, 63.95; H, 3.83. Found: C, 64.00; H, 3.82.

$[(C_5Ph_5)Cr(\mu\text{-}I)I]_2$ (3): I_2 (0.38 g, 3.0 mmol) was dissolved in benzene (50 mL) and transferred via cannula to a flask containing $(C_5Ph_5)Cr(CO)_3$ (1.00 g, 1.72 mmol). The mixture was refluxed overnight, cooled to room temperature, and filtered via cannula. The solid was then dried *in vacuo* to yield **3** as a dark green powder (0.75 g, 58%). mp: 335 °C (dec).[18]

$(C_5Ph_5)CrCl_2(THF)$ (4): $[(C_5Ph_5)Cr(\mu\text{-}Cl)Cl]_2$ (0.25 g, 0.22 mmol) was dissolved in THF (25 mL). After filtering via cannula, the solvent was removed *in vacuo* to yield the product as an olive green powder in near quantitative yield. Microcrystalline samples may be obtained by layering a THF solution of **4** with hexane. Calcd for $C_{39}H_{33}Cl_2CrO$: C, 73.12; H, 5.19. Found: C, 72.56; H, 6.32.

$(C_5Ph_5)CrBr_2(THF)$ (5) and $(C_5Ph_5)CrI_2(THF)$ (6): These compounds are prepared in an analogous fashion to **4**. Calcd for $C_{39}H_{33}Br_2CrO$: C, 64.21; H, 4.56. Found: C, 64.27; H, 4.98.[18]

$(C_5Ph_5)Cr(CO)_3Br$ (7): $(C_5Ph_5)Cr(CO)_3$ (0.50 g, 0.86 mmol) was dissolved in CH_2Cl_2 (30 mL) and cooled to –90 ºC using a liquid nitrogen/acetone bath. Adding bromine (0.041 mL, 1.59 mmol) immediately caused the solution to change from dark blue to dark reddish-brown. This solution was filtered into a second flask and mixed with cold hexane (40 mL). This solution was transferred to a –50 ºC freezer overnight to yield **7** (0.31 g, 55%) as a thermally sensitive, reddish-brown powder.

Results and Discussion

Syntheses. Reaction of the $(C_5Ph_5)Cr(CO)_3$ radical with $C_6H_5I{\bullet}Cl_2$, Br_2, or I_2 yielded olive green complexes of the form $[(C_5Ph_5)Cr(\mu\text{-}X)X]_2$ (X = Cl (**1**), Br (**2**), I (**3**)) in high yields (eq 1).

$$2\ (C_5Ph_5)Cr(CO)_3\ +\ X_2 \xrightarrow{C_6H_6} [(C_5Ph_5)Cr(\mu\text{-}X)X]_2\ +\ 6\ CO \qquad (1)$$

Complex **1** can also be prepared from the reaction of $CrCl_3{\bullet}3THF$ and $Na(C_5Ph_5)$ in refluxing benzene or from the reaction of $CHCl_3$, CCl_4, $SOCl_2$, or PCl_3 with $(C_5Ph_5)Cr(CO)_3$. All three complexes are poorly soluble in non-coordinating solvents, although solubility increases in the order **1** < **2** < **3**. Crystalline materials are produced by layering a solution of the appropriate Me_3SiX in hexane above a solution of a dichloromethane solution of the THF adduct (*vida infra*).[24]

Dissolving these complexes in THF results in their cleavage to monomeric species, $(C_5Ph_5)CrX_2(THF)$ (eq 2). All solids these monomers are very similar in color to their parent

$$[(C_5Ph_5)Cr(\mu\text{-}X)X]_2\ +\ 2\ THF \longrightarrow 2\ (C_5Ph_5)CrX_2(THF)$$

(2)

dimers, but form blue-green solutions. They are much more soluble than their parent dimers.

Initial reaction of $(C_5Ph_5)Cr(CO)_3$ and each halogen results in formation of the expected 18-electron $(C_5Ph_5)Cr(CO)_3X$, which then further reacts with additional halogen to yield $[(C_5Ph_5)CrX_2]_2$. At ambient temperature, solutions of $(C_5Ph_5)Cr(CO)_3I$ decompose over a period of days to **3**, those of $(C_5Ph_5)Cr(CO)_3Br$, **7**, decompose to **2** in less than 10 minutes, and those of $(C_5Ph_5)Cr(CO)_3Cl$ in seconds to **1**. CO stretching frequencies for $(C_5Ph_5)Cr(CO)_3X$ (X = Br, I) are collected in Table 4. Attempts to isolate $(C_5Ph_5)Cr(CO)_3I$ at room temperature always resulted in substantial conversion to $[(C_5Ph_5)CrI_2]_2$. Solutions of $(C_5Ph_5)Cr(CO)_3Br$ prepared and stored below –30 ºC are sufficiently stable that **7** may be isolated as an thermally sensitive, red-brown solid. On standing for several weeks at ambient temperature, this solid converts to $(C_5Ph_5)Cr(CO)_3$ and **2**, presumably via a solid state disproportionation reaction.

The other known $(C_5R_5)Cr(CO)_3X$ (R = H, Me) compounds also exhibit poor stability. King[25] and Baird[26] report that $CpCr(CO)_3Cl$ is quite unstable. Likewise, although $Cp^*Cr(CO)_3X$ (X = Br, I) can be isolated, they decompose slowly in the solid state.[5] Despite being sufficiently stable to isolate, Manning found $CpCr(CO)_3Br$ and $CpCr(CO)_3I$ decompose on gentle heating (76 ºC and 91 ºC, respectively),[15] while King found them too unstable to isolate pure.[25] No decomposition product was identified for any of these compounds. In all cases, the $(C_5Ph_5)Cr(CO)_3X$ compounds are less stable than either their Cp or Cp* analogues. Finally, cyclic voltammetric studies of $[CpCr(CO)_3]_2$ suggest that under appropriate conditions the very unstable $CpCr(CO)_3L^+$ (L = THF, CH_2Cl_2) ion forms, although it was not directly observed.[27]

The C_5Ph_5 ligand probably decreases the stability of the $(C_5Ph_5)Cr(CO)_3X$ complexes relative to their Cp and Cp* analogues because its large size increases crowding and because it releases far less electron density to the metal than either Cp or Cp*.[3,28] Furthermore seven-coordinate first-row transition metal complexes are uncommon because of the small size of the metal atoms/ions.[29]

The aforementioned reports on $(C_5R_5)Cr(CO)_3X$ (X = halide), coupled to reports on the thermal stabilities of X = H[30] and the $[(C_5R_5)Cr(CO)_3]_2$ dimers,[2b,e] suggests that the crowding associated with the 7-coordinate geometry significantly reduces the stabilities of these molecules to a point of marginal viability. However, if only steric factors affected complex stability, the order of stability would be Cl > Br > I. The actual ordering is I > Br > Cl for both R = H and Ph, consistent with electronic factors also playing an important role. A reasonable explanation for this observation posits that as the halogens become more electronegative, the complexes more readily decompose because of decreased electron density available for π-backbonding to the CO ligands.

Molecular Structure of $[(C_5Ph_5)Cr(\mu\text{-}Cl)Cl]_2 \bullet 2CH_2Cl_2$. The X-ray crystal structure of $[(C_5Ph_5)Cr(\mu\text{-}Cl)Cl]_2 \bullet 2CH_2Cl_2$ is displayed in Figure 1. Bond distances and angles are listed in Tables 2 and 3, respectively. The geometry is that of an edge-shared bioctahedron with C_5Ph_5 ligands capping opposite faces and bridging chloride ligands occupying the shared edge. As in $[(C_5H_5)CrCl_2]_2$[11] and $[(C_5Me_5)CrCl_2]_2$,[12] the chromium atoms and bridging chlorines in **1** form a square in the center of the complex. The chromium atoms lie too far apart to bond and their separation is nearly identical in the C_5H_5 and C_5Ph_5 complexes. Bond distances differ only slightly from those in the C_5H_5 and C_5Me_5 complexes. Most bond angles differ between these complexes by 0 – 3º, however, the Cl(bridging)-Cr-Cl(terminal) angles on **1** are 4º – 5º smaller than those on the other complexes. Inspection of a space-filling model of **1** generated from the crystal structure shows close contacts between the terminal chlorine atoms and phenyl rings bound to the Cp on the same chromium atom. These contacts may cause the contraction of the Cr-Cr-Cl bond angle.

Electrochemistry. The electrochemistry of complexes **2** – **6** was investigated by cyclic voltammetry in THF and dichloromethane. $[(C_5Ph_5)CrCl_2]_2$ did not give informative electrochemistry in any solvent. Reduction occurs outside the solvent/electrolyte window and the observed rather positive, irreversible oxidation probably arises from bound chloride.

$[(C_5Ph_5)CrBr_2]_2$ exhibits a quasi-reversible reduction at –0.45 V in dichloromethane.

Incomplete electrochemical reversibility does not allow the number of transferred electrons to be determined from the peak separation. The THF complex, $(C_5Ph_5)CrBr_2(THF)$, displays two successive reductions in the same solvent; the first one reversible and the second irreversible at about –0.5 and –1.4 V, respectively. This pattern more clearly develops after the solution has been kept at ambient temperature for about 30 minutes prior to data collection. Since the first reduction is very close to the one found for the dimeric complex and much different from the reduction pattern of the mononuclear complex in THF (*vide infra*), we suggest complex **5** reverts to dimeric complex **2** in dichloromethane. The observation of two successive reduction peaks then argues for stepwise reduction of each Cr(III) to Cr(II) with concomitant loss of bromide, slower for the first reduction and faster for the second. A large peak at 1.1 V on the successive anodic scan is assigned to the liberation of Br^-.

The mononuclear THF complex, $(C_5Ph_5)CrBr_2(THF)$, in THF instead gave one chemically irreversible reduction, E_{p_c} = –1.04 V, with close lying follow up peaks at –0.23 V and 0.03 V, respectively (Figure 2). Simulation clearly shows these to be direct electrode products of the reduction. Loss of bromide in the course of the reduction is a plausible assumption in this case too, where the follow up peaks are assigned to the reoxidation of the dehalogenated reduction product with and without incorporation of bromide. This conclusion is drawn from the observation that only one single reoxidation (at –0.166 V) follows the –1.04 V reduction on addition of excess Br^- (as $[PPh_3Me]Br$).

Reduction of $(C_5Ph_5)CrI_2(THF)$ in dichloromethane gave very similar electrochemistry to the bromide complex with potentials of –0.75 V and –0.33 V for reduction and reoxidation, respectively. In addition, there are two oxidation peaks at 0.31 V and 0.57 V that occur on the initial anodic scan. The potential range and the fact that the final oxidation is partly reversible argues in favor of a bound iodide, which is liberated at two successive potentials.

Magnetic Susceptibility. The values of χT for all of the mononuclear species, $(C_5Ph_5)CrX_2(THF)$, X = Cl (1.94), Br (1.72), I (1.83) are essentially consistent with the expected spin only value of 1.875 emu-G/mol for d^3 Cr(III) in a pseudo-octahedral field.[31] The data are

temperature independent from 25 K to 250 K with a slight downturn below 25 K and warrant no further comment.

The magnetic properties of $[(C_5Ph_5)CrCl_2]_2$ are illustrated in the plot of χT vs. T (Figure 3). At room temperature, the value of χT is less than that expected for two uncoupled S = 3/2 centers (3.75 emu-G/mol), indicating the presence of antiferromagnetic coupling. This fact has previously been noted by Köhler and co-workers for the corresponding Cp and Cp* analogs, but was apparently never quantified.[12] The data were fit (eq 3) to the analytical solution of the Heisenberg hamiltonian[32] $H = -2J\hat{S}_1 \bullet \hat{S}_2$.

$$\chi T = \frac{2Ng^2\mu_B{}^2}{k}\left\{\frac{\exp[x]+5\exp[3x]+14\exp[6x]}{1+3\exp[x]+5\exp[3x]+7\exp[6x]}\right\} \qquad \text{where x} = \frac{2J}{kT} \tag{3}$$

The two parameter fit gives g = 2.1 and J/k = –30 K. The g value is slightly high compared to the expected value of 2, but the coupling is in the range of other doubly hydroxy-bridged chromium dimers.[33]

Raman Spectroscopy. Due to the sensitivity of the $[(C_5Ph_5)CrX_2]_2$ samples to air and prolonged exposure to high temperature, Raman spectra could only be obtained under low temperature conditions. Solid samples were used because the solid precipitates from solution in liquid samples upon laser exposure. The strongest peaks obtained for each sample are observed in the region containing chromium–halogen and Cp-ring tilting vibrations as seen in Figure 4. All band identifications and assignments are given in Table 5. Samples of $[(C_5Ph_5)Cr(\mu\text{-Br})Br]_2$ (**2**) gave very high scattering backgrounds and did not provide Raman spectra.

The skeletal vibrational modes are designated by the symbol ν, and represent stretching motions. The metal–halogen stretching modes were assigned after those of *trans*-planar $M_2X_4L_2$ and tetrahedral Cp_2MX_2 and $CpMX_3$ compounds (M = a transition metal).[34-37] The ν_b stretches represent stretching of the Cr–X bonds in the $Cr_2(\mu\text{-X})_2$ bridge and occur in the 175–240 and 230–315 cm^{-1} regions in **3** (X = I) and **1** (X = Cl) respectively. These are lower in frequency compared to the terminal Cr–X stretching modes[34] represented by ν_t, which occur at ~283 cm^{-1}

in **3** and ~350 cm^{-1} in **1**. Other halogen-sensitive bands in this region at 131 (**3**) and 157 cm^{-1} (**1**) appear to be X–Cr–X bending (δ) vibrations.[35]

The second Raman region of interest is that containing metal–cyclopentadienyl (Cp) ring stretching and tilting vibrations (400–550 cm^{-1}). Due to the fact that the $[(C_5Ph_5)CrX_2]_2$ compounds are classified in the C_2 point group, the ν(Cr–Cp) stretches can be easily identified as the *A*- and *B*-symmetry modes.[35,36] These two ν(Cr–Cp) modes occur in the narrow range of 400–425 cm^{-1} and are distinguishable in the chloride dimer **1** as seen in Figure 4 and Table 5. However, the *B* mode (~400 cm^{-1}) for the iodide dimer **3** cannot be clearly identified due to close overlap with the *A* mode at 414 cm^{-1}. The Cp ring tilting motions[36] are found in the 450–550 cm^{-1} region. As expected, these Raman bands are almost independent of X and quite similar for both compounds (Figure 4). Finally, the Raman spectra of **1** and **3** taken above 600 cm^{-1} (not shown) also contain internal C_5Ph_5 ligand vibrational modes associated with the Cp and Ph rings at the frequencies typical of centrally π-bonded complexes[34] and monosubstituted benzenes.[38]

Summary. $(C_5Ph_5)Cr(CO)_3$ rapidly reacts with halogens to initially yield $(C_5Ph_5)Cr(CO)_3X$ complexes (X = Cl, Br, I), which then decompose to $[(C_5Ph_5)CrX(\mu\text{-}X)]_2$ dimers in solution. The larger size of C_5Ph_5 (as compared to Cp or Cp*) combined with its reduced tendency to release electron density to metals to which it binds makes the 7-coordinate $(C_5Ph_5)Cr(CO)_3X$ compounds much less stable than their Cp or Cp* analogues. A crystal structure of $[(C_5Ph_5)CrCl_2]_2$ shows the molecule to exhibit only limited intramolecular crowding consistent with the reduced strain in a six-coordinate environment. Magnetic susceptibility measurements show the chromium centers to couple antiferromagnetically. All complexes exhibit complex electrochemical behavior and Raman spectra for the X = Cl and I dimers are assigned. The dimers react with Lewis bases (e.g. THF) to yield monomeric species: $(C_5Ph_5)CrX_2(THF)$.

Acknowledgments. We thank the generous support of the National Science Foundation (Grant NSF CHE-9630094) and the donors of The Petroleum Research Fund, administered by the American Chemical Society for the research at Marshall University. The NSF provided funds towards the University of Delaware diffractometer. GTY thanks the National Institute of

Standards and Technology for the use of the magnetometers and the NSF for support. RSC thanks the Robert A. Welch Foundation (grant E–1184) for support. We also thank Prof. J. W. Larson and Mr. M. M. Dillard for experimental assistance.

Supporting Information Available. For $[(C_5Ph_5)Cr(\mu\text{-}Cl)Cl]_2 \bullet 2CH_2Cl_2$ as follows: Table 1S (bond distances), Table 2S (bond angles), Table 3S (atomic coordinates and equivalent isotropic displacement coefficients), Table 4S (anisotropic displacement coefficients), and Table 5S (hydrogen-atom coordinates) (8 pages). Ordering information is given on any current masthead page.

References

(1) (a) Connelly, N. G.; Geiger, W. C. *Adv. Organomet. Chem.* **1984**, *23*, 1. (b) Baird, M. C. *Chem. Rev.* **1988**, *88*, 1217. (c) Astruc, D. *Chem. Rev.* **1988**, *88*, 1189. (d) *Organometallic Radical Processes*; Trogler, W. C., Ed.; Elsevier: Amsterdam, 1990. (e) Astruc, D. *Electron Transfer and Radical Processes in Transition-Metal Chemistry*; Wiley-VCH: New York, 1995.

(2) (a) Adams, R. D.; Collins, D. E.; Cotton, F. A. *J. Am. Chem. Soc.* **1974**, *96*, 749. (b) McLain, S. J. *J. Am. Chem. Soc.* **1988**, *110*, 643. (c) Goh, L. Y.; Khoo, S. K.; Lim, Y. Y. *J. Organomet. Chem.* **1990**, *399*, 115. (d) Goh, L. Y.; Hambley, T. W.; Darensbourg, D. J.; Reibenspies, J. *J. Organomet. Chem.* **1990**, *381*, 349. (e) Watkins, W. C.; Jaeger, T.; Kidd, C. E.; Fortier, S.; Baird, M. C.; Kiss, G.; Roper, G. C.; Hoff, C. D. *J. Am. Chem. Soc.* **1992**, *114*, 907. (f) The fluorenyl complex $(C_{13}H_9)Cr(CO)_3$ has also been prepared. It is also unstable and undergoes a $Cr(CO)_3$ shift from the C_5 ring to a C_6 ring, followed by a dimerization through the methine C_5 carbon. Novikova, L. N.; Ustynyuk, N. A.; Tumanskii, B. L.; Petrovskii, P. V.; Borisenko, A. A.; Kukharenko, S. V.; Strelets, V. V. *Isv. Akad. Nauk, Ser. Khim.* **1995**, 1354 (Engl. Transl. *Russ. Chem. Bull.* **1995**, *44*, 1306).

(3) Hoobler, R. J.; Hutton, M. A.; Dillard, M. M.; Castellani, M. P.; Rheingold, A. L.; Rieger, A. L.; Rieger, P. H.; Richards, T. C.; Geiger, W. E. *Organometallics* **1993**, *12*, 116.

(4) Hackett, P.; O'Neill, P.S.; Manning, A. R. *J. Chem. Soc., Dalton Trans.* **1974**, 1625.

(5) Jaeger, T. J.; Baird, M. C. *Organometallics* **1988**, *7*, 2074.

(6) Goulin, C. A.; Huber, T. A.; Nelson, J. M.; Macartney, D. H.; Baird, M. C. *J. Chem. Soc., Chem. Commun.* **1991**, 798.

(7) Huber, T. A.; Macartney, D. H.; Baird, M. C. *Organometallics* **1995**, *14*, 592.

(8) MacConnachie, C. A.; Nelson, J. A.; Baird, M. C. *Organometallics* **1992**, *11*, 2521.

(9) Scheer, M.; Nam, T. T.; Schenzel, K.; Herrmann, E.; Jones, P. G.; Fedin, V. P.; Ikorski, V. N.; Fedorov, V. E. *Z. Anorg. Allg. Chem.* **1990**, *591*, 221.

(10) Richeson, D. S.; Mitchell, J. F.; Theopold, K. H. *Organometallics* **1989**, *8*, 2570.

(11) Köhler, F. H.; de Cao, R.; Ackermann, K.; Sedlmair, J. *Z. Naturforsch.* **1983**, *38B*, 1406.

(12) Köhler, F. H.; Lachmann, J.; Müller, G.; Zeh, H.; Brunner, H.; Pfauntsch, J.; Wachter, J. *J. Organomet. Chem*. **1989**, *365*, C15.

(13) Morán, M. *Trans. Met. Chem.* **1981**, *6*, 173.

(14) Fischer, E. O.; Ulm, K.; Kuzel, P. *Z. Anorg. Allg. Chem*. **1963**, *319*, 253.

(15) Manning, A. R.; Thornhill, D. J. *J. Chem. Soc. (A)* **1971**, 637.

(16) Collman, J. P.; Kittleman, E. T. *Inorg. Syn.* **1966**, *8*, 149.

(17) Lucas, H. J.; Kennedy, E. R. *Organic Syntheses*; Wiley, 1955; Collect. Vol. 3, p 482.

(18) In our experience, samples containing the C_5Ph_5 ligand frequently exhibit poor elemental analyses. This occurs even for samples where other analytical techniques are consistent with a pure sample. Duplicate analyses can sometimes differ by more than 5% in carbon. For this reason, no elemental analyses are reported for the iodo compounds. The syntheses and the physical and spectroscopic properties measured were consistent with the formulations given.

(19) Kölle, U.; Kossakowski, J. *Inorg. Chim. Acta* **1989**, *164*, 23.

(20) Gosser, D. K. In *Cyclic Voltammetry*; VCH: Weinheim, 1994.

(21) Czernuszewicz, R. S.; Johnson, M. K. *Appl. Spectrosc*. **1983**, *37*, 297-300.

(22) Czernuszewicz, R. S. In *Methods in Molecular Biology*, Jones, C.; Mulloy, B.; Thomas, A. H., Eds.; Humana Press: Totawa, 1993, Vol. 17, p 345.

(23) Sellers, S. P.; Korte, B. J.; Fitzgerald, J. P.; Reiff, W. M., Yee, G. T. *J. Am. Chem. Soc.* **1998**, *120*, 4662.

(24) van der Heijden, H.; Schaverien, C. J.; Orpen, A. G. *Organometallics* **1989**, *8*, 255.

(25) King, R. B.; Efraty, A.; Douglas, W. M. *J. Organomet. Chem*. **1973**, *60*, 125.

(26) MacConnachie, C. A.; Nelson, J. M.; Baird, M. C. *Organometallics* **1992**, *11*, 2521.

(27) O'Callaghan, K. A. E.; Brown, S. J.; Page, J. A.; Baird, M. C.; Richards, T. C.; Geiger, W. E. *Organometallics* **1991**, *10*, 3119.

(28) (a) Broadley, K.; Lane, G. A.; Connelly, N. G.; Geiger, W. E. *J. Am. Chem. Soc.* **1983**, *105*, 2486. (b) Connelly, N. G.; Geiger, W. E.; Lane, G. A.; Raven, S. J.; Rieger, P. H. *J. Am. Chem. Soc.* **1986**, *108*, 6219. (c) Lane, G. A.; Geiger, W. E.; Connelly, N. G. *J. Am. Chem. Soc.* **1987**, *109*, 402. (d) Connelly, N. G.; Manners, I. *J. Chem. Soc., Dalton Trans.* **1989**, 283.

(29) Huheey, J. E.; Keiter, E. A.; Keiter, R. L. *Inorganic Chemistry: Principles of Structure and Reactivity, 4th Edition*; Harper Collins: New York, 1993; p. 502.

(30) (a) Fischer, E. O. *Inorg. Syn*. **1963**, *7*, 136. (b) Wormsbächer, D.; Nicholas, K. M.; Rheingold, A. L. *J. Chem. Soc., Chem. Commun*. **1985**, 721. (c) Leoni, P.; Landi, A.; Pasquali, M. *J. Organomet. Chem*. **1987**, *321*, 365.

(31) Bender-Gresse, M.; Collange, E.; Poli, R., Mattamana, S. *Polyhedron* **1998,** *17*, 1115.

(32) Carlin, R. L. *Magnetochemistry*; Springer-Verlag: Berlin, 1986; p. 94.

(33) Michelsen, K.; Pederson, E.; Wilson, S. R.; Hodgson, D. J. *Inorg. Chem. Acta* **1982**, *63*, 141.

(34) Nakamoto, K. In *Infrared and Raman Spectra of Inorganic and Coordination Compounds, Part B*; 5th ed.; John Wiley: New York, 1997; p 188.

(35) Maslowsky, E.; Nakamoto, K. *Appl. Spectrosc.* **1971**, *25*, 187.

(36) Samuel, E.; Ferner, R.; Bigorgne, M. *Inorg. Chem.* **1973**, *12*, 881.

(37) Balducci, G.; Bencivenni, L.; DeRosa, G.; Gigli, R.; Martini, B.; Cesaro, S. N. *J. Mol. Struct*. **1980**, *64*, 163.

(38) Dollish, F. R.; Fateley, W. G.; Bentley, F. F. *Characteristic Raman Frequencies of Organic Compounds*, Wiley-Interscience: New York, 1974; p 162.

Table 1. Crystal and Refinement Data for $[(C_5Ph_5)Cr(\mu\text{-}Cl)Cl]_2 \cdot 2CH_2Cl_2$.

a. Crystal Data

formula	$C_{72}H_{54}Cl_8Cr_2$
fw	1306.8
cryst system	triclinic
space group	$P\bar{1}$
a, Å	12.072 (6)
b, Å	12.290 (6)
c, Å	12.638 (6)
α, deg	67.23 (4)
β, deg	65.28 (4)
γ, deg	75.99 (2)
V, Å^3	1565 (5)
Z	1
color	dark green
crystal size, mm	0.42 x 0.44 x 0.48
D (Calcd), g/cm^3	1.362
abs coeff, mm^{-1}	0.732

b. Data Collection

diffractometer	Siemens P3m/V
radiation	MoKα (λ =0.710 73 Å)
temp, K	296
2θ scan range, deg	4.0 to 48.0
scan type	Wycoff
reflns collcd	5191
obsd rflns	2868 ($F > 5.0\sigma(F)$)

c. Solution and Refinement

solution	direct methods
refinement method	full-matrix least-squares
quantity minimized	$\Sigma w(F_o - F_c)^2$
weighting scheme	$w^{-1} = \sigma^2(F) + 0.0010F^2$
number of parameters refined	311
final *R* indices (obs. data), %	$R = 6.73$, $wR = 8.25$
R indices (all data), %	$R = 11.19$, $wR = 9.32$
GOF	1.58
data-to-parameter ratio	9.2:1
largest difference peak, eÅ^{-3}	0.75
largest difference hole, eÅ^{-3}	-0.61

Table 2. Selected Bond Distances (Å) in $[(C_5Ph_5)Cr(\mu\text{-}Cl)Cl]_2 \cdot 2CH_2Cl_2$.

	$[(C_5Ph_5)Cr(\mu\text{-}Cl)Cl]_2$[a]	$[(C_5H_5)Cr(\mu\text{-}Cl)Cl]_2$[b]	$[(C_5Me_5)Cr(\mu\text{-}Cl)Cl]_2$[c]
Cr-C(1)	2.270 (5)		
Cr-C(2)	2.285 (5)		
Cr-C(3)	2.266 (6)		
Cr-C(4)	2.240 (7)		
Cr-C(5)	2.242 (7)		
Cr-CNT[d]	1.911	1.867	1.88
Cr-Cl(1)	2.247 (3)	2.274 (2)	2.291 (2)
Cr-Cl(2)	2.380 (3)	2.377 (1)	2.393 (1)
Cr-Cl(2A)	2.360 (3)	2.374 (1)	2.383 (1)
Cr(A)-Cl(2)	2.360 (3)		
Cr-Cr	3.375	3.362 (1)	

[a]This work.

[b]Ref. 11.

[c]Ref. 12. There were two conformers in the unit cell. Averaged values are presented.

[d]CNT = centroid of the cyclopentadienyl ring

Table 3. Selected Bond Angles (°) in $[(C_5Ph_5)Cr(\mu\text{-}Cl)Cl]_2 \cdot 2CH_2Cl_2$.

	$[(C_5Ph_5)Cr(\mu\text{-}Cl)Cl]_2$[a]	$[(C_5H_5)Cr(\mu\text{-}Cl)Cl]_2$[b]	$[(C_5Me_5)Cr(\mu\text{-}Cl)Cl]_2$[c]
Cl(1)-Cr-Cl(2)	92.2 (1)	96.12 (6)	97.0 (1)
Cl(1)-Cr-Cr(2A)	92.2 (1)		96.5 (1)
Cl(2)-Cr-Cl(2A)	89.2 (1)	89.89 (5)	87.7 (1)
Cr-Cl(2)-Cr(A)	92.2 (1)		92.3 (1)
CNT-Cr-Cl(1)	124.4	123.6	123.2
CNT-Cr-Cl(2)[d]	124.6	121.8	122.0
CNT-Cr-Cl(2A)[d]	124.2	120.5	122.4

[a]This work.

[b]Ref. 11.

[c]Ref. 12. There were two conformers in the unit cell. Averaged values are presented.

[d]CNT = centroid of the cyclopentadienyl ring

Table 4. Infrared Spectral Data for $(C_5Ph_5)Cr(CO)_3X$ Complexes

complex	solvent	ν(C≡O), cm^{-1}	reference
$(C_5H_5)Cr(CO)_3Br$	CS_2	2041, 1986, 1954	15
$(C_5Me_5)Cr(CO)_3Br$	hexane	2032, 1979, 1935	5
$(C_5Ph_5)Cr(CO)_3Br$[a]	THF	2031, 1980 , 1939	this work
$(C_5H_5)Cr(CO)_3I$	CS_2	2029, 1975, 1953	15
$(C_5Me_5)Cr(CO)_3I$	hexane	2018, 1967, 1934	5
$(C_5Ph_5)Cr(CO)_3I$	THF	2016, 1965, 1937	this work

[a]A cold solution of $(C_5Ph_5)Cr(CO)_3Br$ was rapidly transferred to an IR cell at ambient temperature and the spectrum was immediately taken.

Table 5. Raman Low-Frequencies (cm^{-1}) and Assignments for $[(C_5Ph_5)Cr(\mu\text{-}X)X]_2$ Complexes ($X = Cl^-, I^-$)

$[(C_5Ph_5)CrCl_2]_2$	$[(C_5Ph_5)CrI_2]_2$	assignment
157	131	δ(X–Cr–X)
231	177	ν_b(Cr–X)
255	198	ν_b(Cr–X)
272, 311	240	ν_b(Cr–X)
351	283, 275	ν_t(Cr–X)
421	414	ν(Cr–Cp), *A*
401	400 sh	ν(Cr–Cp), *B*
482 br	490 br	Cp ring tilt
536	530	Cp ring tilt

Figure Captions

Figure 1. Molecular structure and labeling scheme for $[(C_5Ph_5)Cr(\mu\text{-}Cl)Cl]_2 \bullet 2CH_2Cl_2$ (**1**) (30% thermal ellipsoid probability).

Figure 2. Cyclic voltammograms of $(C_5Ph_5)CrBr_2(THF)$; A: in THF at v = 100 mV/s, B: same after addition of $[PPh_3Me]Br$.

Figure 3. Plot of χT vs. T for $[(C_5Ph_5)CrCl_2]_2$ and fit to Heisenberg hamiltonian model.

Figure 4. Low-temperature (77 K) Raman spectra (100–600 cm^{-1}) of **1** (*bottom*) and **3** (*top*) excited at 514.5 nm. Both spectra obtained via backscattering on KCl pellets in a liquid-N_2 dewar; (**1**) 400 mW laser power, 6 cm^{-1} slit widths, average of 16 scans; (**3**) 150 mW laser power, 8 cm^{-1} slit widths, average of 15 scans.

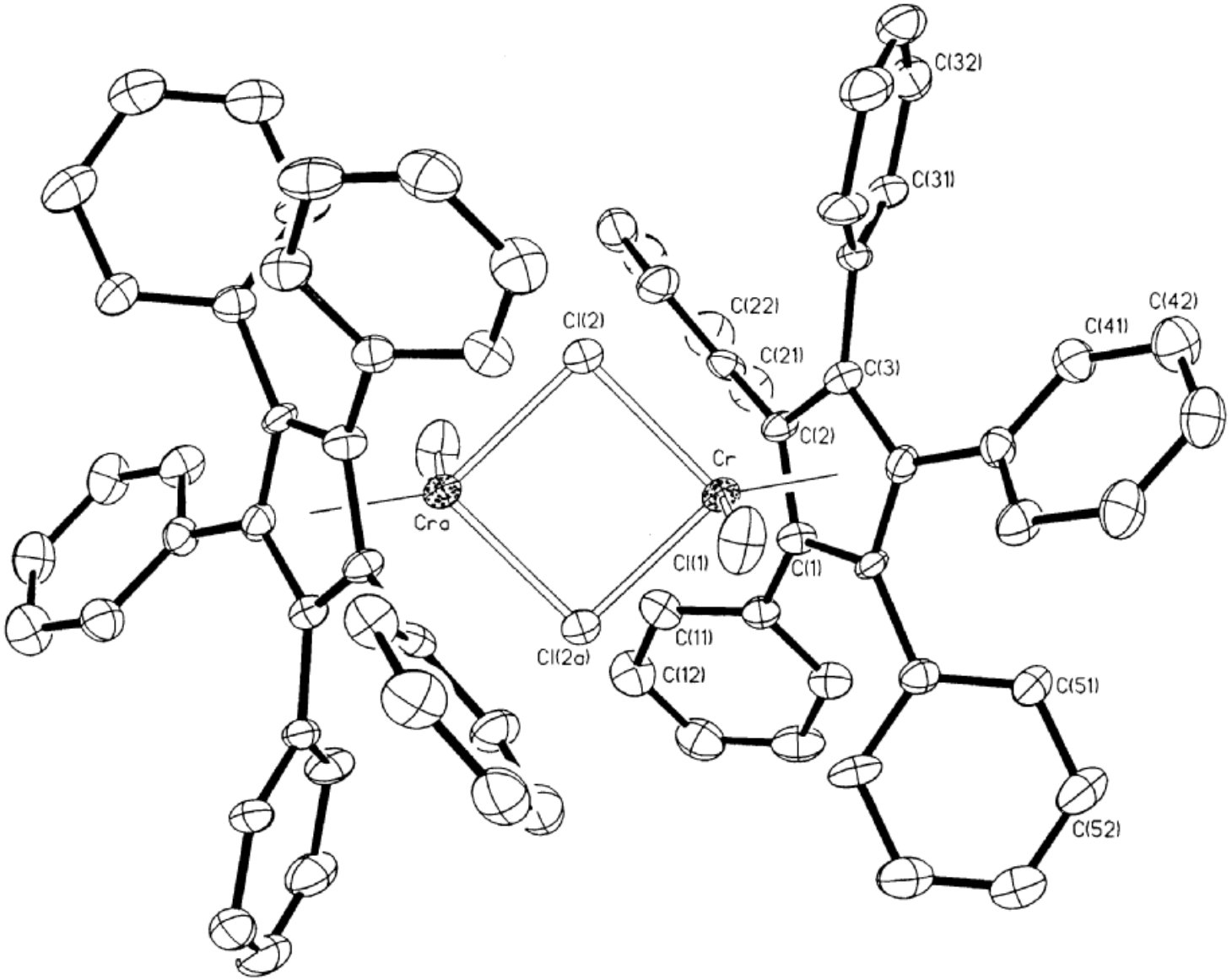
C(32)
C(31)
C(22)
C(21)
C(3)
C(2)
C(41)
C(42)
Cl(2)
Cr
Cra
Cl(1)
C(1)
Cl(2a)
C(11)
C(12)
C(51)
C(52)

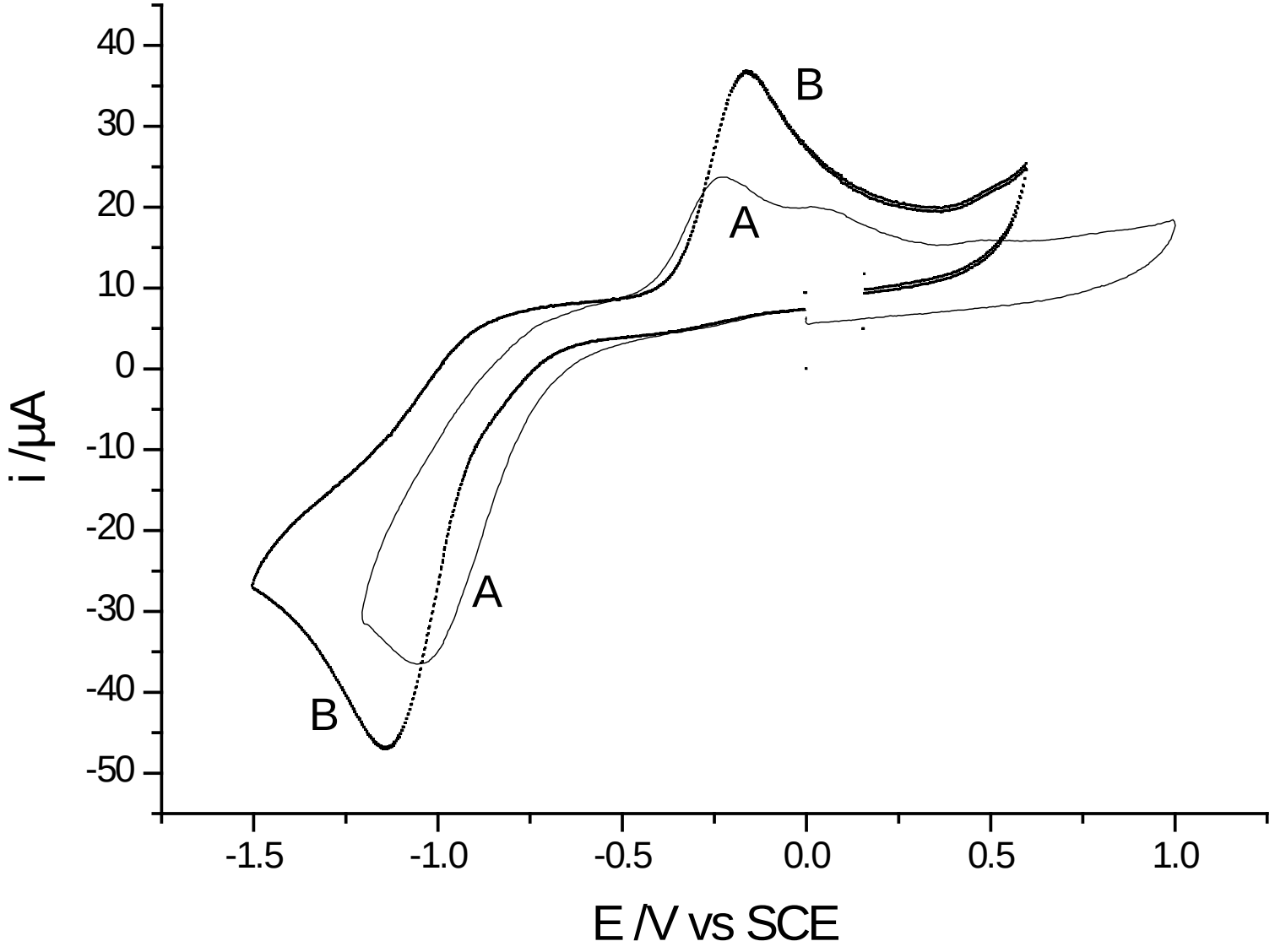
40
30
20
10
0
-10
-20
-30
-40
-50
i /µA
B
A
A
B
-1.5
-1.0
-0.5
0.0
0.5
1.0
E /V vs SCE

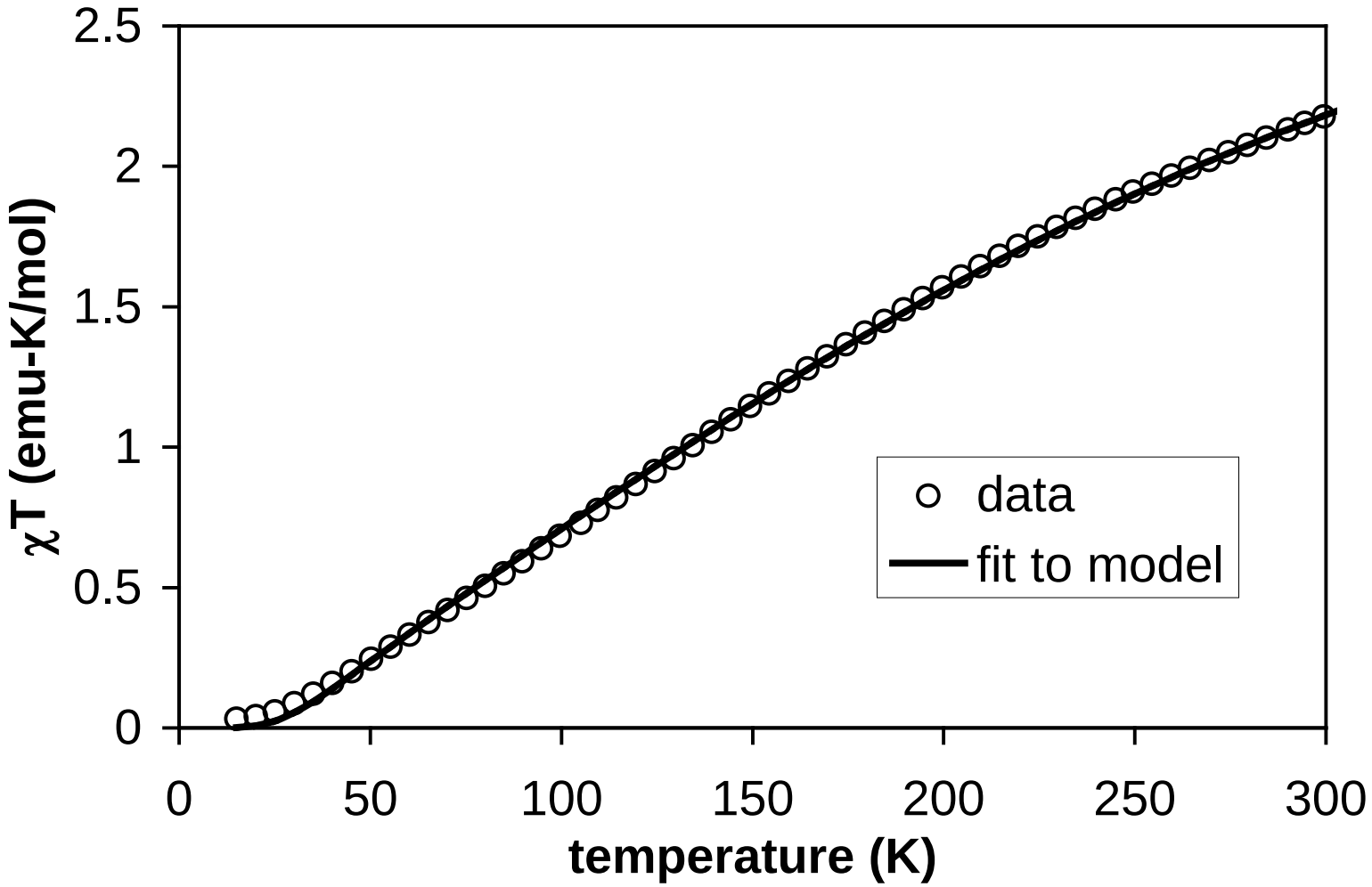
2.5
2
1.5
1
0.5
0
χT (emu-K/mol)
0
50
100
150
200
250
300
temperature (K)
data
fit to model

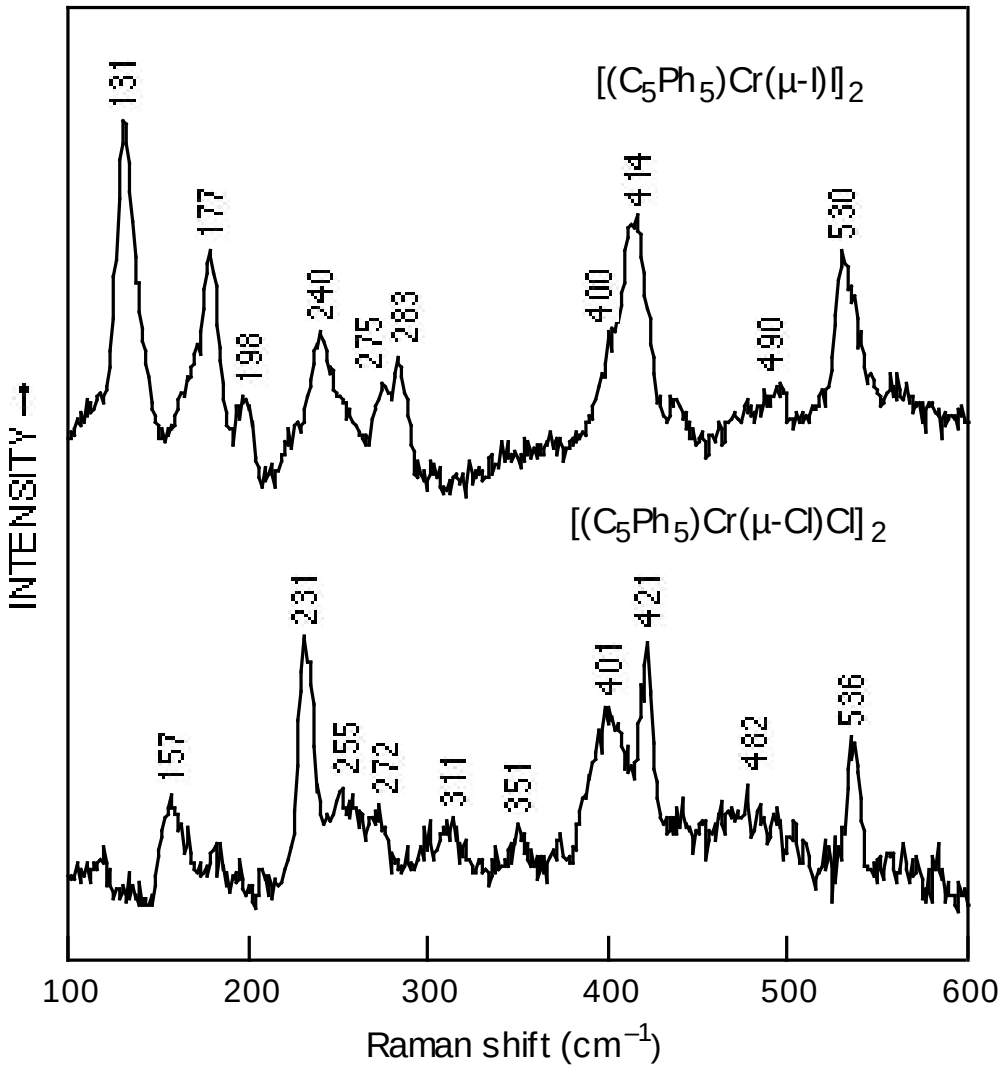
[(C5Ph5)Cr(μ-I)I]2
131
177
198
240
275
283
400
414
490
530
[(C5Ph5)Cr(μ-Cl)Cl]2
157
231
255
272
311
351
401
421
482
536
INTENSITY →
100
200
300
400
500
600
Raman shift (cm−1)

Supporting Information

for

Halogen Oxidation Reactions of $(C_5Ph_5)Cr(CO)_3$ and Lewis Base Addition To $[(C_5Ph_5)Cr(\mu\text{-}X)X]_2$: Electrochemical, Magnetic, and Raman Spectroscopic Characterization of $[(C_5Ph_5)CrX_2]_2$ and $(C_5Ph_5)CrX_2(THF)$ (X = Cl, Br, I). X-ray Crystal Structure of $[(C_5Ph_5)Cr(\mu\text{-}Cl)Cl]_2$

Marc A. Hutton, James C. Durham, Robert W. Grady, Brett E. Harris, Carter S. Jarrell, J. Matthew Mooney, Michael P. Castellani*, Arnold L. Rheingold* , Ulrich Kölle*, Brenda J. Korte, Roger D. Sommer, Gordon T. Yee*

Table 1S. Bond Distances (Å) in $[(C_5Ph_5)CrCl(\mu\text{-}Cl)]_2 \cdot 2CH_2Cl_2$.

Cr-C(1)	2.270 (5)
Cr-C(2)	2.285 (5)
Cr-C(3)	2.266 (6)
Cr-C(4)	2.240 (7)
Cr-C(5)	2.242 (7)
Cr-CNT[d]	1.911
Cr-Cl(1)	2.247 (3)
Cr-Cl(2)	2.380 (3)
Cr-Cl(2A)	2.360 (3)
Cr(A)-Cl(2)	2.360 (3)
Cr-Cr	3.375
C(1)-C(16)	1.473 (5)
C(2)-C(26)	1.494 (7)
C(3)-C(36)	1.490 (6)
C(4)-C(46)	1.475 (7)
C(5)-C(56)	1.502 (7)
C(90)-Cl(3)*	2.099 (44)
C(90)-Cl(4)*	1.897 (31)

*C(90) refers to the carbon in the dichloromethane. Likewise, Cl(3) and Cl(4) refer to the chlorine atoms in the solvate.

Table 2S. Bond Angles (º) in $[(C_5Ph_5)Cr(\mu\text{-}Cl)Cl]_2 \cdot 2CH_2Cl_2$.

Cl(1)-Cr-Cl(2)	92.2 (1)	Cl(1)-Cr-C(3)	118.0 (1)
Cl(1)-Cr-Cr(2A)	92.2 (1)	Cl(1)-Cr-C(4)	92.9 (1)
Cl(2)-Cr-Cl(2A)	89.2 (1)	Cl(1)-Cr-C(5)	102.9 (1)
Cr-Cl(2)-Cr(A)	92.2 (1)	Cl(2)-Cr-C(3)	96.5 (2)
CNT-Cr-Cl(1)	124.4	Cl(2)-Cr-C(4)	126.4 (1)
CNT-Cr-Cl(2)	124.6	Cl(2)-Cr-C(5)	157.2 (1)
CNT-Cr-Cl(2A)	124.2	C(1)-Cr-Cl(2A)	92.1 (1)
Cl(1)-Cr-C(1)	138.0 (2)	C(2)-Cr-Cl(2A)	112.6 (1)
Cl(1)-Cr-C(2)	153.1 (2)	C(3)-Cr-Cl(2A)	148.9 (1)
Cl(2)-Cr-C(1)	129.6 (1)	C(4)-Cr-Cl(2A)	143.7 (1)
Cl(2)-Cr-C(2)	98.3 (2)	C(5)-Cr-Cl(2A)	107.1 (1)
C(1)-Cr-C(2)	36.3 (1)	Cr-C(1)-C(16)	129.9 (4)
C(1)-Cr-C(3)	60.9 (2)	Cr-C(2)-C(26)	132.1 (4)
C(1)-Cr-C(4)	61.3 (2)	Cr-C(3)-C(36)	125.5 (4)
C(1)-Cr-C(5)	36.7 (1)	Cr-C(4)-C(46)	131.6 (3)
C(2)-Cr-C(3)	36.4 (1)	Cr-C(5)-C(56)	125.7 (4)
C(2)-Cr-C(4)	61.0 (2)	C(1)-C(16)-C(11)	120.1
C(2)-Cr-C(5)	61.0 (2)	C(2)-C(26)-C(21)	118.2
C(3)-Cr-C(4)	36.7 (1)	C(3)-C(36)-C(31)	118.7
C(3)-Cr-C(5)	61.3 (2)	C(4)-C(46)-C(41)	118.6
C(4)-Cr-C(5)	36.9 (1)	C(5)-C(56)-C(51)	116.9
Cr-C(1)-C(2)	72.4 (1)	C(1)-C(16)-C(15)	119.9
Cr-C(2)-C(1)	71.3 (1)	C(2)-C(26)-C(25)	121.7
Cr-C(2)-C(3)	71.1 (1)	C(3)-C(36)-C(35)	120.9
Cr-C(3)-C(2)	72.5 (1)	C(4)-C(46)-C(45)	121.3

Cr-C(3)-C(4)	70.6 (1)	C(5)-C(56)-C(55)	122.8
Cr-C(4)-C(3)	72.7 (1)	C(5)-C(4)-C(46)	125.9
Cr-C(4)-C(5)	71.6 (1)	C(5)-C(1)-C(16)	124.3
Cr-C(5)-C(4)	71.4 (1)	C(1)-C(2)-C(26)	126.7
Cr-C(1)-C(5)	70.6 (1)	C(4)-C(3)-C(36)	125.8
Cr-C(5)-C(1)	72.7 (1)	C(3)-C(4)-C(46)	124.8
C(2)-C(1)-C(16)	127.0	C(1)-C(5)-C(56)	124.5
C(3)-C(2)-C(26)	124.3	C(4)-C(5)-C(56)	126.4
C(2)-C(3)-C(36)	126.0	Cl(3)-C(90)-Cl(4)	90.7 (16)

Table 3S. Atomic Coordinates (x10^4) and Equivalent Isotropic Displacement Coefficients ($Å^2$ x 10^3) for $[(C_5Ph_5)Cr(\mu\text{-}Cl)Cl]_2 \cdot 2CH_2Cl_2$.

	x	*y*	*z*	*U(eq)*[a]
Cr	60(1)	983(1)	603(1)	28(1)
Cl(1)	267(2)	-444(2)	2297(2)	56(1)
Cl(2)	-1516(2)	61(2)	699(2)	36(1)
C(1)	820(3)	2737(5)	-704(3)	29(3)
C(2)	-457	2883	-462	28(3)
C(3)	-1086	2695	818	29(3)
C(4)	-199	2433	1367	28(4)
C(5)	980	2459	426	26(3)
C(11)	1839(4)	2600(4)	-2819(4)	38(4)
C(12)	2763	2887	-3981	49(5)
C(13)	3665	3578	-4245	55(5)
C(14)	3643	3984	-3346	54(5)
C(15)	2719	3698	-2183	38(4)
C(16)	1817	3006	-1920	29(4)
C(21)	-658(4)	4406(4)	-2369(4)	42(4)
C(22)	-1239	4931	-3222	56(5)
C(23)	-2223	4426	-3099	56(5)
C(24)	-2624	3396	-2123	50(5)
C(25)	-2042	2871	-1270	42(4)
C(26)	-1059	3377	-1393	30(4)
C(31)	-3092(4)	3909(4)	1057(4)	38(4)
C(32)	-4338	4101	1715	53(5)
C(33)	-4933	3214	2777	59(6)
C(34)	-4282	2134	3180	60(5)

C(35)	-3035	1942	2521	42(4)
C(36)	-2440	2829	1460	29(4)
C(41)	-1349(4)	3256(4)	3071(4)	44(4)
C(42)	-1575	3300	4231	53(5)
C(43)	-922	2496	4948	53(5)
C(44)	-43	1648	4505	49(5)
C(45)	184	1604	3345	39(4)
C(46)	-469	2407	2628	32(4)
C(51)	2316(4)	3092(4)	1075(5)	40(4)
C(52)	3446	3097	1129	59(6)
C(53)	4444	2335	676	60(5)
C(54)	4311	1570	170	61(5)
C(55)	3182	1565	116	45(4)
C(56)	2184	2327	569	32(4)
C(90)	3213(16)	-312(21)	3282(20)	202(16)
Cl(3)	5120(35)	-595(21)	2816(27)	132(14)
Cl(3')	4355(24)	-1202(25)	3103(12)	237(12)
Cl(4)	3043(4)	307(5)	4510(5)	174(4)

[a]Equivalent isotropic *U* defined as one third of the trace of the orthogonalized $\mathbf{U}_{ij}$ tensor.

Table 4S. Anisotropic Displacement Coefficients ($Å^2x10^3$).

	U_{11}	U_{22}	U_{33}	U_{12}	U_{13}	U_{23}
Cr	25(1)	32(1)	28(1)	-5(1)	-12(1)	-7(1)
Cl(1)	93(2)	40(1)	44(1)	-11(1)	-43(1)	-1(1)
Cl(2)	26(1)	41(1)	43(1)	-6(1)	-8(1)	-18(1)
C(1)	22(4)	36(5)	24(4)	-2(3)	-7(3)	-6(3)
C(2)	23(4)	40(5)	23(4)	-10(3)	-6(3)	-9(3)
C(3)	27(4)	27(4)	30(4)	-5(3)	-14(3)	-3(3)
C(4)	30(4)	30(4)	33(4)	-2(3)	-17(4)	-11(3)
C(5)	18(4)	39(5)	28(4)	-6(3)	-9(3)	-13(3)
C(11)	37(5)	39(5)	29(4)	-8(4)	-6(4)	-4(4)
C(12)	61(6)	50(6)	31(5)	-14(5)	-8(4)	-12(4)
C(13)	40(5)	58(6)	44(6)	-10(5)	1(4)	-9(5)
C(14)	29(5)	65(6)	48(6)	-22(4)	-4(4)	0(5)
C(15)	34(4)	37(5)	39(5)	-5(4)	-11(4)	-9(4)
C(16)	28(4)	27(4)	30(4)	0(3)	-13(3)	-5(3)
C(21)	48(5)	35(5)	37(5)	-2(4)	-19(4)	-2(4)
C(22)	65(6)	56(6)	38(5)	3(5)	-28(5)	-3(5)
C(23)	62(6)	58(7)	57(6)	21(5)	-41(5)	-21(5)
C(24)	46(5)	60(6)	58(6)	6(5)	-30(5)	-28(5)
C(25)	35(5)	55(6)	37(5)	-5(4)	-19(4)	-10(4)
C(26)	27(4)	34(5)	25(4)	8(3)	-11(3)	-10(3)
C(31)	25(4)	46(5)	43(5)	1(4)	-14(4)	-16(4)
C(32)	44(5)	66(7)	65(6)	16(5)	-33(5)	-36(5)
C(33)	30(5)	104(9)	54(6)	-3(5)	-15(5)	-39(6)
C(34)	37(5)	92(8)	44(5)	-28(5)	-2(4)	-16(5)

C(35)	23(4)	55(6)	35(5)	-4(4)	-3(4)	-9(4)
C(36)	18(4)	47(5)	27(4)	0(3)	-9(3)	-18(4)
C(41)	46(5)	51(6)	37(5)	-1(4)	-18(4)	-14(4)
C(42)	59(6)	53(6)	46(6)	3(5)	-17(5)	-21(5)
C(43)	74(6)	59(6)	32(5)	-11(5)	-22(5)	-16(5)
C(44)	65(6)	51(6)	33(5)	-8(5)	-26(4)	-7(4)
C(45)	43(5)	45(5)	31(5)	-4(4)	-17(4)	-10(4)
C(46)	33(4)	35(5)	29(4)	-4(4)	-10(4)	-14(4)
C(51)	33(4)	45(5)	47(5)	-4(4)	-15(4)	-19(4)
C(52)	49(6)	84(8)	61(6)	-25(5)	-28(5)	-21(6)
C(53)	35(5)	75(7)	71(7)	-6(5)	-23(5)	-21(6)
C(54)	35(5)	70(7)	71(7)	7(5)	-16(5)	-28(6)
C(55)	31(5)	57(6)	56(6)	-2(4)	-27(4)	-16(5)
C(56)	28(4)	39(5)	28(4)	-3(4)	-12(3)	-7(4)
C(90)	111(14)	205(23)	183(20)	7(14)	-48(14)	25(17)
Cl(3)	107(18)	98(14)	165(19)	14(11)	-55(14)	-25(11)
Cl(3')	168(16)	217(18)	223(10)	83(16)	-53(9)	-46(10)
Cl(4)	110(3)	202(6)	157(4)	-6(3)	-49(3)	-9(4)

The anisotropic displacement factor exponent takes the form: $-2\pi^2(h^2a^{*2}U_{11} + ... + 2hka^*b^*U_{12})$

Table 5S. H-Atom Coordinates ($x10^4$) and Isotropic Displacement Coefficients ($Å^2x10^3$).

	x	y	z	U
H(11)	1217	2124	-2637	80
H(12)	2778	2608	-4600	80
H(13)	4301	3776	-5045	80
H(14)	4264	4460	-3528	80
H(15)	2704	3977	-1565	80
H(21)	19	4754	-2454	80
H(22)	-963	5639	-3893	80
H(23)	-2623	4787	-3686	80
H(24)	-3301	3048	-2038	80
H(25)	-2319	2163	-599	80
H(31)	-2682	4520	326	80
H(32)	-4787	4844	1438	80
H(33)	-5792	3346	3230	80
H(34)	-4691	1523	3910	80
H(35)	-2587	1199	2799	80
H(41)	-1798	3809	2577	80
H(42)	-2181	3883	4536	80
H(43)	-1078	2526	5746	80
H(44)	407	1095	4998	80
H(45)	789	1020	3040	80
H(51)	1630	3616	1387	80
H(52)	3537	3624	1478	80
H(53)	5221	2338	713	80
H(54)	4998	1046	-142	80
H(55)	3091	1038	-233	80

For Table of Contents Use Only

Halogen Oxidation Reactions of $(C_5Ph_5)Cr(CO)_3$ and Lewis Base Addition To $[(C_5Ph_5)Cr(\mu\text{-}X)X]_2$: Electrochemical, Magnetic, and Raman Spectroscopic Characterization of $[(C_5Ph_5)CrX_2]_2$ and $(C_5Ph_5)CrX_2(THF)$ (X = Cl, Br, I). X-ray Crystal Structure of $[(C_5Ph_5)Cr(\mu\text{-}Cl)Cl]_2$

Reaction of halogens ($X_2 = Cl_2$, Br_2, and I_2) with $(C_5Ph_5)Cr(CO)_3$ yields the series of complexes $[(C_5Ph_5)Cr(\mu\text{-}X)X]_2$. The reaction proceeds through $(C_5Ph_5)Cr(CO)_3X$ intermediates, that decompose to $[(C_5Ph_5)CrX_2]_2$. Lewis bases cleave these dimers to the monomeric species $(C_5Ph_5)CrX_2L$. X-ray crystallography, electrochemistry, magnetic susceptibility, and Raman spectroscopy were used to characterize the complexes.

For Table of Contents Use Only